

# Buckling versus Folding: Importance of Viscoelasticity

S.M. Schmalholz and Yu. Podladchikov

Geologisches Institut, ETH Zentrum, CH-8092 Zurich, Switzerland

**Abstract.** We present a dominant wavelength solution for a viscoelastic layer embedded in a low viscosity matrix under layer-parallel compression based on the thin-plate approximation. We show that the deformation mode approximates the elastic or viscous limits depending on a parameter,  $R$ , which is the ratio of dominant wavelength predicted by pure viscous theory to the one predicted by pure elastic theory. In contrast, conventional analyses based on the Deborah number incorrectly predict the deformation mode. The dominant viscoelastic wavelength closely follows the minimum out of viscous and elastic dominant wavelengths. The viscoelastic thin-plate theory is verified by two-dimensional modeling of large strain viscoelastic folding, for which we develop a new numerical algorithm based on a combined spectral/finite-difference method. The robustness of the numerical code is demonstrated by calculation, for the first time, of the pressure field evolution during folding of a viscoelastic layer with up to 100% strain.

## Introduction

Buckling and folding instabilities are common modes of rocks deformation at all scales (e.g. [Ramsay and Huber, 1987]). Two thin-plate analytical theories exist to describe either the buckling of a pure elastic layer or folding of a pure viscous layer embedded in a low viscosity matrix (e.g. [Biot, 1961; Turcotte and Schubert, 1982]). The applicability of the pure viscous solution is limited to viscosity contrasts between layer and matrix of less than two orders of magnitude. The pure elastic theory is also problematic in that it requires an unrealistically high ratio of layer-parallel stress to the layer's shear modulus to fit observed buckling wavelengths. Moreover, the application either theory demands knowledge of the deformation mode (viscous folding or elastic buckling) which cannot be known a priori or may change during deformation. The viscoelastic solution presented in this paper resolves these problems of the end-member solutions. The importance of the combined treatment of viscous and elastic effects to predict the mode of instability development and stress field evolution was

reported for similar problems of Rayleigh-Taylor and compaction-driven fluid flow instabilities (e.g. [Connolly and Podladchikov, 1998; Vasilyev et al., 1998] and references therein) and for viscoelastic single-layer buckling (e.g. [Zhang et al., 1996; Mancktelow, 1999]).

## Analytical thin-plate solution for viscoelastic folding

A viscoelastic layer with a small sinusoidal perturbation embedded in an infinite, low viscosity matrix subject to layer-parallel shortening is considered. The thin-plate theories assume a linear variation of the fiber stress across the layer,  $\sigma_{xx}(x, y, t)$ , as (cf. [Turcotte and Schubert, 1982])

$$\sigma_{xx} \approx -P(t) + \tau(t)y \cos(2\pi x/\lambda) \quad (1)$$

where  $t$  is the time,  $x$  and  $y$  are the coordinates along and across the layer, respectively,  $P$  is the layer-parallel stress,  $\tau$  is the coefficient in linear dependence of the bending stresses as a function of  $y$  and  $\lambda$  is the wavelength of a sinusoidal perturbation. Typically, thin-plate theories assume an exponential growth of the amplitude of the sinusoidal perturbations,  $h = h_0 \exp(\alpha t)$ , where  $h_0$  and  $\alpha$  are the initial amplitude and growth factor, respectively. The growth factor reaches a maximum for a certain wavelength, which is designated the dominant wavelength (e.g. [Turcotte and Schubert, 1982]). Most folds observed in nature are thought to record dominant wavelengths. The aforementioned analytical viscous and elastic thin-plate theories predict "viscous" and "elastic" dominant wavelengths, which in the incompressible case (Poisson ratio is equal 0.5) are given by  $2\pi H 6^{-1/3} (\mu_l/\mu_m)^{1/3}$  and  $2\pi H (G/P)^{1/2}$ , respectively (cf. [Turcotte and Schubert, 1982]). Here,  $H$ ,  $\mu_l$ ,  $\mu_m$  and  $G$  are the thickness of the layer, the viscosity of the layer, the viscosity of the matrix and the shear modulus of the layer, respectively. The viscous dominant wavelength solution, only reproduces natural wavelengths (usually smaller 30, e.g. [Currie et al., 1962; Sherwin and Chapple, 1968]) if the viscosity contrast is smaller than around 500. This limitation of the viscous model is a significant shortcoming given that experimental observations (e.g. [Carter and Tsenn, 1987]) on power law creep suggest that in natural environments effective viscosity (stress/strain rate) contrasts may exceed four orders of magnitude. Furthermore, the applicability of the elastic solution is also limited in that the solution requires  $P/G > 0.1$  to obtain real-

Copyright 1999 by the American Geophysical Union.

Paper number 1999GL900412.  
0094-8276/99/1999GL9000412\$05.00

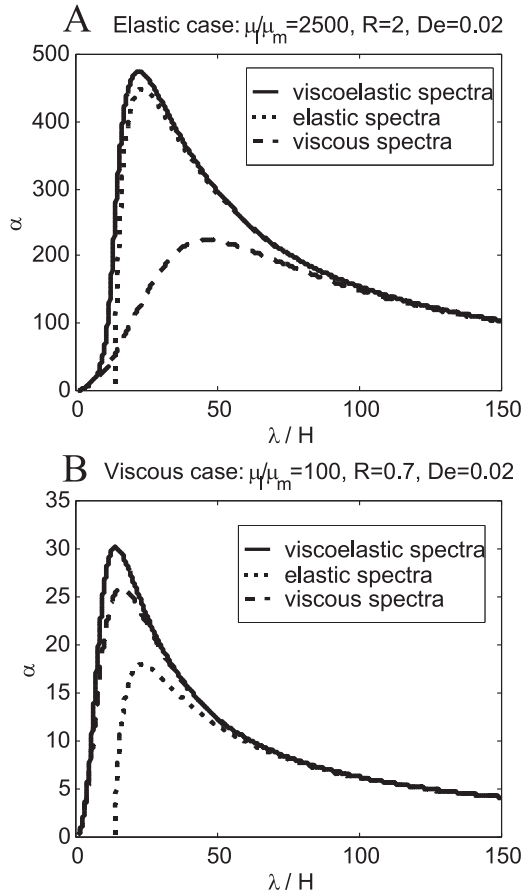


**Figure 1.** Viscoelastic thin-plate predictions for the growth factor versus normalized wavelength of the sinusoidal perturbation. A) Although the Deborah number (De) is small, which implies viscous behavior, the viscoelastic curve is close to elastic ( $\lambda_{dve}/H = 22$ ). B) De is unchanged but the viscoelastic curve is close to the viscous one ( $\lambda_{dve}/H = 14$ ). Importantly,  $R > 1$  for A) and  $R < 1$  for B).  $P_0/G$  is 0.07 in both cases.

istic dominant wavelengths. Large  $P/G$  ratios are unreasonable, because rocks cannot sustain such stresses compared to the shear modulus. We describe folding of a viscoelastic layer with two differential equations: the bending equation (stress equilibrium equation), and the constitutive equation for a linear viscoelastic material (Maxwell model, cf. [Turcotte and Schubert, 1982]). The constitutive equation is written for the fiber stress  $\sigma_{xx}$ . This equation is split into an equation for the stress coefficient  $\tau$  and an equation for the layer-parallel stress  $P$  by collecting terms independent on  $y$  coordinate and linearly scaling with  $y$ . Dimensional analysis (e.g. [Barenblatt, 1996]) using  $\mu_l/G$ ,  $h_0$ ,  $P_0$  and  $4h_0w^2G$  as characteristic time, length, layer-parallel stress and coefficient of the bending stresses, respectively, results in 3 non-dimensional initial conditions ( $h=1$ ,  $P=1$  and  $\tau=0$ ), and a system of 3 ordinary differential equations (ODE's):

$$-\frac{\partial h}{\partial t} + \frac{\partial \tau}{\partial t} + \tau = 0 \tag{2}$$

$$-\frac{4\mu_l e}{P_0} + \frac{\partial P}{\partial t} + P = 0 \tag{3}$$

$$-\tau + 3R^2\lambda_V^2hP - 2\lambda_V^3\frac{\partial h}{\partial t} = 0 \tag{4}$$

where

$$R = \frac{\lambda_{dv}}{\lambda_{de}} = 6^{-\frac{1}{3}} \left(\frac{\mu_l}{\mu_m}\right)^{\frac{1}{3}} \left(\frac{P_0}{G}\right)^{\frac{1}{2}}; \lambda_V = \frac{\lambda}{\lambda_{dv}}$$

$e$  is the background strain rate. The parameter  $R$  we designate as the dominant wavelength ratio. Solving the system of ODE's provides three growth factors. Two of them determine viscoelastic adjustment of initial stresses on the Maxwell time scale,  $\mu_l/G$ . After a transient period of several Maxwell time scales the solution is dominated by the third “folding“ growth factor,

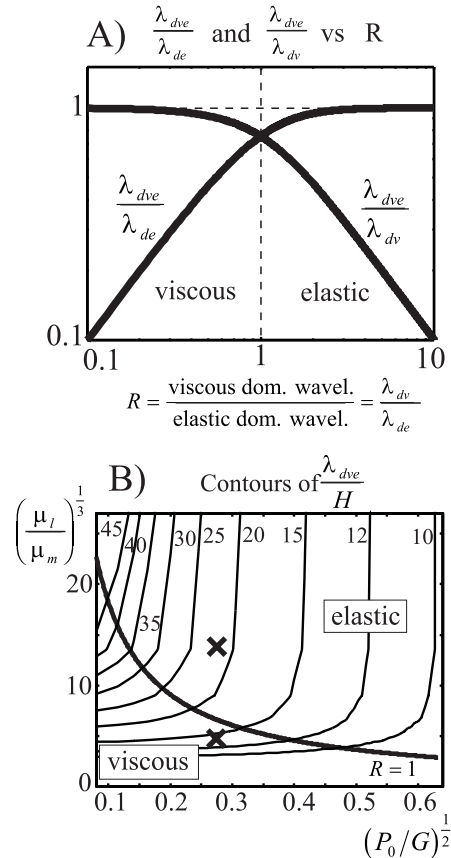


**Figure 2.** Analytical thin-plate predictions for the viscoelastic dominant wavelength  $\lambda_{dve}$ . A) The ratios of  $\lambda_{dve}$  over  $\lambda_{dv}$  and  $\lambda_{de}$  versus  $R$  (log-log plot). For  $R < 1$   $\lambda_{dv} \approx \lambda_{dve}$ , whereas for  $R > 1$   $\lambda_{de} \approx \lambda_{dve}$ . There is a sharp transition from the viscous to the elastic mode around  $R=1$ . B) The “phase diagram“ of folding versus buckling shows contours of  $\lambda_{dve}/H$  in the  $\mu_l/\mu_m$ - $P_0/G$  space. The line for  $R=1$  separates the viscous and elastic domains. The two crosses mark the locations of the two  $\lambda_{dve}/H$  shown in Fig. 1.

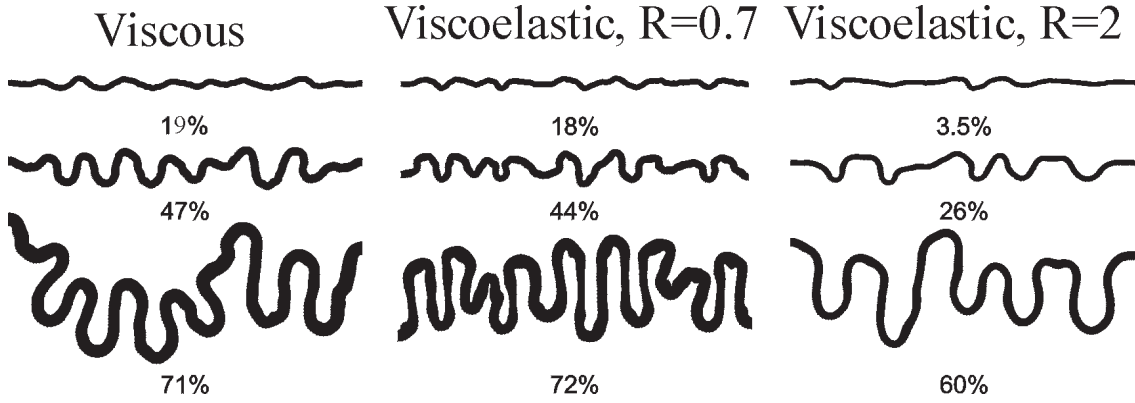


**Figure 3.** Numerical simulation of the development of the predicted dominant wavelengths. Initially, all layers had initial random perturbation with the same amplitude and the same aspect ratio of 1:128. In the viscous case  $\lambda_{dv}/H = 16$  and therefore eight ( $128/16=8$ ) folds are developed. For  $R=0.7$  the predicted  $\lambda_{dve}/H = 14$  and nine folds are observed, whereas for  $R=2$   $\lambda_{dve}/H = 22$  and five folds are developed. The dominant wavelength is predicted by the dominant wavelength ratio  $R$  but not by the Deborah number, which is the same for the viscoelastic cases.

which is positive, real and depends only on  $R$  and  $\lambda_V$ :

$$\alpha = \frac{3}{4} \frac{R^2}{\lambda_V} - \frac{1}{2} - \frac{1}{4\lambda_V^3} + \frac{1}{4\lambda_V^3}$$

$$\sqrt{9R^4\lambda_V^4 + 6R^2(2\lambda_V^5 - \lambda_V^2) + 4(\lambda_V^6 + \lambda_V^3) + 1} \quad (5)$$

The ratio of the characteristic time scale for viscoelastic stress relaxation,  $\mu_l/G$ , to the characteristic time scale of the deformation,  $1/e$ , is the Deborah number, which is conventionally employed to discriminate viscous versus elastic behavior ( $De = \mu_l e/G$ ). In this paper we focus on small Deborah numbers,  $De \sim 0.01$ , which is normally interpreted to imply viscous behavior. This allows us to neglect the transient evolution and to use steady state values for the layer-parallel stress ( $P_0 = 4\mu_l e$ ) and the amplification factor (equation (5)) in the analysis of the dominant wavelength selection. Fig. 1A and B show plots of  $\alpha$ 's obtained from the viscous, elastic and viscoelastic solutions versus  $\lambda/H$ . In Fig. 1A the viscoelastic solution is close to elastic whereas in Fig. 1B the viscoelastic solution is close to viscous, although  $De$  is the same in both cases. The controlling parameter is  $R$ , which is smaller one in the viscous and larger one in the elastic case. The reason for the failure of predictions based on the Deborah number is that the background strain rate is a bad estimator for the characteristic rates of folding in systems with high viscosity contrasts. In Fig. 2A the ratios  $\lambda_{dve}/\lambda_{dv}$  and  $\lambda_{dve}/\lambda_{de}$  are plotted versus  $R$ . The mode which produces a ratio closest to one controls the deformation and a sharp transition occurs around  $R=1$ . In Fig. 2B  $\lambda_{dve}/H$  is contoured in the  $\mu_l/\mu_m - P_0/G$  space.  $\lambda_{dve}/H$  in the area below the  $R=1$  line is strongly dependent on the viscosity contrast (the viscous mode), whereas  $\lambda_{dve}/H$  in the area above the  $R=1$  line is strongly dependent on  $P_0/G$  (the elastic mode).

### Spectral/Finite-Difference simulation of viscoelastic folding

Viscoelastic folding is simulated in 2D, for plane strain, in the absence of gravity and for incompressible materials. The following three partial differential equations are set up for four unknown functions  $v_1$ ,  $v_2$ ,  $\tau_{11}$  and  $\tau_{12}$  which are velocities in the x- and y-directions, deviatoric stress in the x-direction, and the shear stress, respectively.

$$2\tau_{11,12} + \tau_{12,22} - \tau_{12,11} = 0 \quad (6)$$

$$v_{i,j} + v_{j,i} = \tau_{ij}/\mu + \dot{\tau}_{ij}/G; i, j = 1, 2 \quad (7)$$

$$v_{1,1} + v_{2,2} = 0 \quad (8)$$

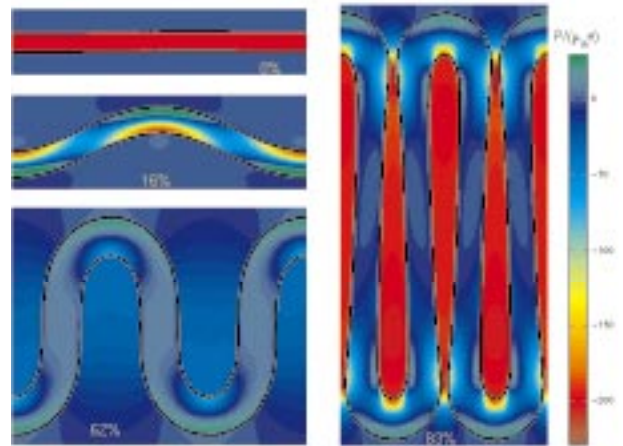


**Figure 4.** Results of numerical modeling of pressure field evolution ( $R=0.5$ ).  $P$  is normalized with  $\mu_m e$  and negative areas represent compressive pressures. Strong pressure gradients between top and bottom of the fold hinge are developing during shortening (16%). At 62% shortening there are no big pressure differences between the layer and the matrix. Note high pressure buildup within the matrix between the limbs (83%).

Equation (6) is the equilibrium equation, (7) is the Maxwell equation, where  $\tau_{ij}$  is the upper convected derivative (e.g. [Huilgol and Phan-Thien, 1997]), and (8) is the continuity equation.

For the numerical simulation the time derivatives are approximated with finite differences (FD's) implicit in time using a variable time step,  $dt$ . We take advantage of the periodic behavior in the shortening (x-) direction and approximate the x-dependence with a spectral method (e.g. [Canuto et al., 1988]). The non-periodic behavior in the amplification (y-) direction is approximated with a conservative FD method using a variable, staggered grid. The 2D numerical code was verified versus our viscoelastic thin-plate solution at small strains. Three numerical simulations of the folding of single layers with an initial aspect ratio of 1:128 (thickness/length) are shown in Fig. 3. These simulations were conducted using 1001 grid points and 64 harmonics. The initial perturbations of the layer boundaries were generated by an equally distributed pseudo-random sequence with the same amplitude (1:50th of the layer thickness) for all three cases. The dominant wavelengths are controlled by  $R$ , but not by  $De$ .

Fig. 4 shows the pressure ( $P(x,y,t)$ , not the layer-parallel stress  $P$  for the thin-plate model!) field during shortening for viscoelastic behavior ( $R=0.5$ ). The computed pressure field is free of the artificial oscillations typical of spectral methods and viscoelastic solvers in Eulerian formulation.

## Conclusions

Our dominant wavelength ratio  $R$  determines whether viscoelastic layers show nearly viscous or elastic behavior, whereas analyses based on conventional Deborah number yields false predictions as shown in Fig. 1. Realistic dominant wavelengths can be obtained with our viscoelastic solution for high viscosity contrasts and relatively small ratios of  $P_0/G$  (Fig. 2). Our finite amplitude numerical simulations of shortening of initially randomly perturbed layers confirm development of the dominant wavelength predicted by the parameter  $R$  (Fig. 3). The robustness of the numerical code is demonstrated by calculation, for the first time, of the pressure field evolution during buckling of a viscoelastic layer with up to 100% strain. Success of our Eulerian formulation allows us to model folding up to very large strain and to monitor the transition of the high pres-

sure areas from inside the layer to the matrix between the fold limbs at the later stages of folding (Fig. 4). Success of our Eulerian formulation allows us to model folding up to very large strain.

**Acknowledgments.** We thank D. Yuen and K. Wang for reviews and J. Connolly for improving English of the paper. S. Schmalholz was supported by ETH project Nr. 0-20-499-98.

## References

- Barenblatt, G. I. *Scaling, self-similarity, and intermediate asymptotics*, Cambridge University Press, Cambridge, 1996.
- Biot, M. A., Theory of folding of stratified viscoelastic media and its implications in tectonics and orogenesis, *Geol. Soc. America Bull.* 72, 1595-1620, 1961.
- Canuto, C., M.Y. Hussaini, A. Quarteroni, and T.A. Zang *Spectral Methods in Fluid Dynamics*, Springer, Berlin Heidelberg, 1988.
- Carter, N.L., and M.C. Tsenn, Flow properties of continental lithosphere, *Tectonophysics* 136, 27-63, 1987.
- Connolly, J.A.D., and Y.Y. Podladchikov, Compaction-driven fluid flow in viscoelastic rock, *Geodinamica Acta* 11, 55-84, 1998.
- Currie, I.B., H.W. Patnode, and R.P. Trump, Development of folds in sedimentary strata, *Geol. Soc. Am. Bull.* 73, 655-674, 1962.
- Huilgol, R.R., and N. Phan-Thien *Fluid mechanics of viscoelasticity: General principles, constitutive modeling, analytical and numerical techniques*, Elsevier, Amsterdam, 1997.
- Mancktelow, N.S., Finite-element modelling of single-layer folding in elasto-viscous materials: the effect of initial perturbation geometry, *J. Struct. Geol.* in press, 1999.
- Ramsay, J.G., and M.I. Huber *The techniques of modern structural geology. Volume 2: Folds and fractures*, Academic Press, London, 1987.
- Sherwin, J., and W.M. Chapple, Wavelengths of single layer folds: a comparison between theory and observation, *Am. Jour. Sci.* 266, 167-179, 1968.
- Turcotte, D.L., and G. Schubert *Geodynamics. Applications of continuum physics to geological problems*, John Wiley, 1982
- Vasilyev, O.V., Y.Y. Podladchikov, and D.A. Yuen, Modeling of compaction driven flow in poro-viscoelastic medium using adaptive wavelet collocation method, *Geophys. Res. Lett.* 17, 32-39, 1998.
- Zhang, Y., B.E. Hobbs, and A. Ord, Computer simulation of single-layer buckling, *J. Struct. Geol.* 18, 643-655, 1996.

Yu. Podladchikov and S. M. Schmalholz, Geologisches Institut, ETH Zentrum, CH-8092 Zurich, Switzerland, (e-mail: stefan@erdw.ethz.ch)

(Received July 30, 1998; revised February 2, 1999; accepted March 8, 1999.)